

## Characterization of Microtearing modes in RFX-mod plasma

S. Spagnolo<sup>1,2</sup>, M. Zuin<sup>2</sup>, I. Predebon<sup>2</sup>, F. Sattin<sup>2</sup>, R. Cavazzana<sup>2</sup>, A. Fassina<sup>2</sup>, M. Gobbin<sup>2</sup>, E. Martines<sup>2</sup>, B. Momo<sup>2</sup>, M. Spolaore<sup>2</sup>, N. Vianello<sup>2</sup>

<sup>1</sup>*Centro Ricerche Fusione, Università di Padova, Italy*

<sup>2</sup>*Consorzio RFX, Associazione EURATOM-ENEA, Padova, Italy*

Microtearing (MT) modes have been observed for the first time in the RFX-mod reversed-field pinch (RFP) [1]. Coherent high frequency magnetic activity, associated to wavelengths of the order of few ion gyroradii, has been detected in correspondence of the presence of strong temperature gradients, as expected by gyrokinetic calculations [2].

In the RFX-mod device internal temperature barriers are observed to arise during Quasi Single Helicity (QSH) states [3], when the ( $m=1, n=7$ ) tearing mode, being  $m$  and  $n$  poloidal and toroidal mode numbers, dominates over the others. The QSH

helical equilibrium is characterized by recurrent transitions to the Multiple Helicity states (MH), where all tearing modes have comparable amplitudes. This dynamics can be recognized in Fig. 1 where the red line represents the time evolution of the toroidal magnetic field fluctuation  $B_\phi^{(1,7)}$  at the edge during the flat top phase of a typical high current discharge.

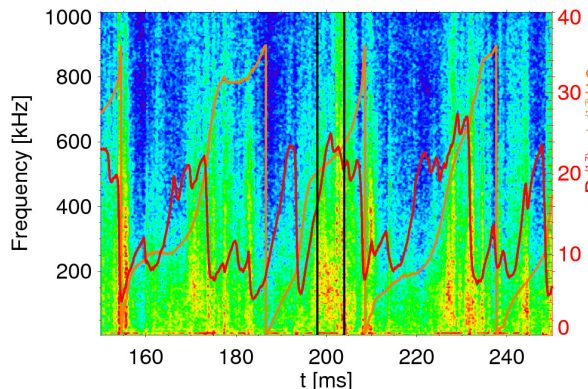


**Fig. 1: Spectrogram  $S(f,t)$  of the poloidal fluctuation signal. The red and the orange curve represent respectively the amplitude  $B_\phi^{(1,7)}$  and the phase of the dominant tearing mode. The black lines indicate the time range investigated hereafter.**

In the figure, the spectrogram of the magnetic fluctuation is shown. Experimental data are provided by in-vessel magnetic sensors, with high space and time resolution, measuring magnetic field fluctuations along the three spatial dimensions (radial, poloidal and toroidal). Magnetic fluctuations recognized as Microtearing modes have been detected at frequencies of about 100-200 kHz, on the signal of the poloidal component. Due to

the structure of the RFP field, this turns out to be related to perpendicular component of fluctuations resonant in the core [4].

Moreover, it can be noticed that the mode can be measured by the edge probes only at some fixed phase values of the dominant mode (orange line in Fig. 1), because of the helical shape of the equilibrium that makes the plasma asymmetric: MT are observed when the ridge of the helix passes in front of the measuring probe (corresponding to phase values in the range  $\varphi_{\phi}^{(1,7)} \approx 170^\circ \div 300^\circ$ ). The black lines identify a time range where the above-mentioned conditions are satisfied and the mode can be observed and studied. In particular, in this paper our purpose is to get new informations about the relation between the mode and the temperature barriers and to verify the effect of the magnetic shear on MT characteristics. With this aim, the poloidal and toroidal mode numbers behavior has been analyzed, focusing both on their time evolution during a single shot, but also on a statistical basis.

The two-point technique [5] has been applied to the signals from sensors in different

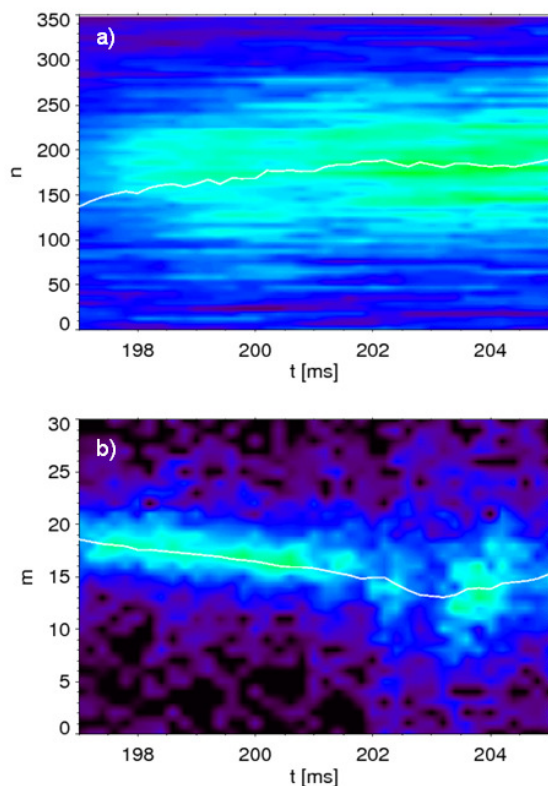


**Fig. 2: Time evolution of toroidal (a) and poloidal (b) mode numbers. The color code represents the amplitude of the modes (in a.u.). White lines indicate the maximum of the  $S(n)$  and  $S(m)$  spectra amplitude.**

toroidal and poloidal positions, in order to characterize the high poloidal and toroidal mode numbers (respectively, in the ranges  $m \approx 5 \div 25$  and  $n \approx 50 \div 250$ ) of the modes and to study their time evolution, as shown in Fig. 2. It can be observed that, while the value of  $n$  is slightly growing in the time interval of interest,  $m$  visibly decreases. In other cases, where the increase of the toroidal mode value is clearer, the poloidal one exhibits a weaker change. The overall consequence is that the safety factor value where the mode is resonant,  $q_s = m/n$ , has a gradual reduction in time. In Fig. 3, the evolution of the  $q(r)$  profiles obtained by the SHEq code [6] is shown at the instants under analysis. It is worth noting that the resonance is moving

outwards, as indicated by vertical lines.

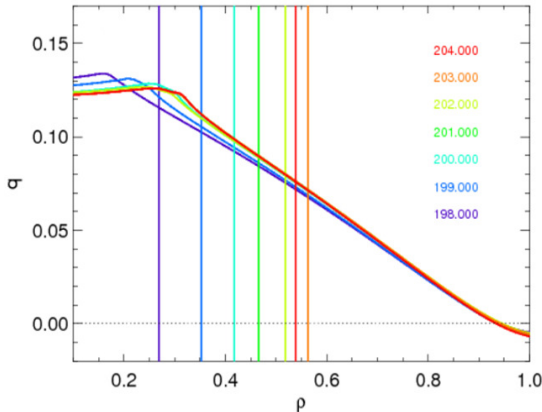


**Fig. 4:** Helical  $q$  profiles at different times; for each one a vertical line indicates the radial position where the MT mode resonates.

gradients grow with the dominant mode during the rising phase, while turn out to be less steep during the QSH flattop phase [7]. For these reason, at the moment, we limit our analysis to the first phase only. Anyway, the role of the MT modes during flattop phases is currently under investigation since they could turn out to be a good candidate to explain the loss of the thermal barrier before the QSH crash.

In Fig. 4a the dynamics of the poloidal mode number is shown. The black line represents the position of the temperature gradient estimated as explained in [7]; the red one is the amplitude of the dominant mode. It is worth noting that when the  $B_\phi^{(1,7)}$  rises,

the temperature barriers move outwards, in accordance with the evolution of the resonance position (although only qualitatively), as previously underlined. This behavior is statistically confirmed comparing the position of the temperature barrier  $r_{Te}$  and the position of the MT resonance  $r_s$ , selecting the rising phases of the

In order to understand this behavior, the time evolution of the temperature barriers measured by a multi-chord double filter SXR spectrometer [7] has been analyzed. It has been observed a different behavior of the temperature gradient during the *rising* phase of the QSH intervals (when the dominant mode rises) and the *flattop* phase (when it approximately remains at a high level). In particular, the temperature

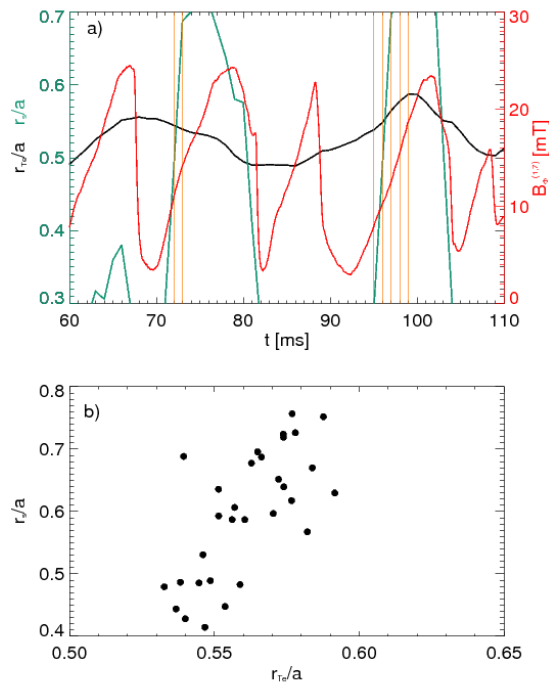


**Fig. 3:** a) Time evolution of the temperature barrier position (black line) and of the MT resonance position (green line); the red one represents the dominant (1,7) mode amplitude. Orange vertical lines indicate the time instants inserted in the bottom plot (b), where relative positions are statistically compared.

dominant mode and the suitable phase angles,  $\varphi_\phi^{(1,7)}$  (e.g. the instants are indicated by the orange vertical lines). In Fig. 4b, even if the statistics at the moment is small, the corresponding positions are observed to move in the same direction.

From a theoretical point of view, the role of the  $q$  profile in MT mode destabilization is rather important: the growth rate increases as  $q$  or the magnetic shear  $s = \frac{q' r}{q}$  decreases (where  $q' = \frac{dq}{dr}$ ); furthermore, the wave-numbers increase as  $s$  decrease.

For this reason, the effect of the magnetic shear on the observed wavelengths has been investigated. The experimental results are summarized in Fig. 5, where the values of poloidal and toroidal mode numbers measured by the in-vessel probes are plotted *vs* the parameter  $s$ . In particular, it can be distinguished an almost linear trend of  $n$  values and a clear inverse relation between  $m$  values measured and the corresponding shear. This behavior underlines the strong contribution of the  $1/q$  factor in the shear definition. The comparison with theoretical predictions, provided by GS2 code simulations, is only partial at the moment, since the parameters  $q$  and  $s$  are considered to vary independently one from the other. Further analysis in order to better reproduce the experimental settings is in progress.

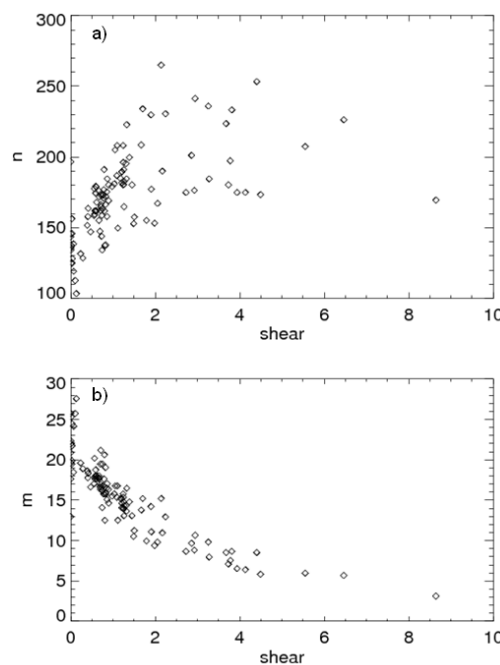


**Fig. 5 Toroidal (a) and poloidal (b) mode numbers associated to the measured MT modes *vs* magnetic shear.**

*This work, supported by the European Communities under the contract of Association between EURATOM/ENEA, was carried out within the framework of the European Fusion Development Agreement.*

## References

- [1] P. Sonato, et al., *Fus. Eng. Des.* **66** 161 (2003)
- [2] I. Predebon, et al., *Phys. Rev. Lett.* **105** 195001 (2010)
- [3] R. Lorenzini, et al., *Nature Phys.* **5** 570 (2009)
- [4] M. Zuin, et al., *Phys. Rev. Lett.* **110** 055002 (2013)
- [5] J.M. Beall, et al., *J. Appl. Phys.* **53** 3933 (1982)
- [6] B. Momo et al., *Plasma Phys. Control Fusion* **53** (2011) 125004
- [7] P. Franz, et al., *Nucl. Fusion* **53** 053011 (2013)